Available online at www.sciencedirect.com
ScienceDirect
Journal of Sound and Vibration 299 (2007) 1–11
JOURNAL OF SOUND AND VIBRATION
www.elsevier.com/locate/jsvi

Dynamic analysis of layered composite shells using nine node degenerate shell elements

S. Jayasankar, S. Mahesh, S. Narayanan, Chandramouli Padmanabhan*

Machine Design Section, Department of Mechanical Engineering, Indian Institute of Technology Madras, Chennai 600036, India

Received 22 December 2004; received in revised form 8 June 2006; accepted 12 June 2006
Available online 20 September 2006

Abstract

The basic objective of the work reported in this paper is to extend a nine-node degenerated shell element developed earlier for stress analysis to the free vibration analysis of thick laminated composites. The nine-noded degenerated shell element is preferable to conventional solid elements for the modeling and analysis of laminated composite shell structures since the shell element works for both thick and thin shells. An enhanced interpolation of the transverse shear strains in the natural coordinates is used in this formulation to produce a shear locking free element and an enhanced interpolation of the membrane strains in the local coordinates is used to produce a membrane locking free element. The interpolation functions used in formulating the assumed strains are based on the Lagrangian interpolation polynomials. Various numerical examples are analyzed and their results are compared with the existing exact solutions where available and the numerical solutions calculated from other shell finite element formulations, to benchmark the current formulation.

1. Introduction

Laminated composites shell and plate structures are widely used in many branches of engineering because of their high strength to weight ratio, low specific gravities and modulus to weight ratio. The importance of composite shell structures and analysis complexity leads to the use of finite element (FE) method for the solution of many types of problems. In engineering practice it is of vital importance to conduct the dynamic analysis of structures so as to use the information in the design process. Large number of thin shell elements has been developed to meet the demands in different industries. In the context of FE analysis, numerous elements have been proposed for the analysis of shell like structures. These range from simple flat plate elements to more sophisticated doubly curved elements based on thin shell theory. Three-dimensional (3-D) elements were used initially to analyze thick shell structures. Ahmad et al. [1] put forward the degenerated solid approach for thick shells. The degeneration concept directly discretizes the 3-D field equation in terms of mid-surface nodal variables. However, it was found that there were serious defects such as locking phenomena in the degenerated shell element. Zienkiewicz et al. [2] improved the degenerated shell element by reducing the order of numerical integration, to eliminate shear and membrane locking. Pawsey et al. [3] applied selective integration procedure to the degenerated shell element to eliminate shear

*Corresponding author. Tel.: +91 44 2257 8192; fax: +91 44 2257 0509.
E-mail address: mouli@iitm.ac.in (C. Padmanabhan).

0022-460X/$ - see front matter © 2006 Elsevier Ltd. All rights reserved.
doi:10.1016/j.jsv.2006.06.058

and membrane locking. However, shell elements with reduced integration suffered from mechanisms. Huang and Hinton [4] proposed the assumed strain method to avoid locking phenomena. This assumed strain method has been used successfully in stress calculations. Lee et al. [5] extended the nine-noded degenerate shell element for free vibration analysis. He used the assumed natural strain method to eliminate the locking phenomena. It can be seen that there have been few investigations on the performance of nine noded assumed strain degenerated shell elements to laminated shells under free and forced vibrations.

In this paper a nine noded degenerated shell element formulation for dynamic analysis of laminated plates and shells is provided with emphasis on terms related to laminated composite stiffness and mass matrices. Numerical validation has been done using existing exact solutions and numerical solutions from other shell FE formulations. The geometry of the shell is represented by the coordinates and normal vectors of its middle surface [1]. The middle surface is modeled by the degenerate isoparametric element in 3-D space. The element used in the formulation is a nine-node Lagrangian element. Each node has five degrees-of-freedom (dof), three translations and two rotations with respect to the axes in the plane of the middle surface. The independent rotational and displacement dof permit transverse shear deformation to be taken into account. The global coordinates of the pairs of points on the top and bottom surface at each node are used to define the geometry. Different coordinate systems are adopted in the degenerated shell element formulation (see Fig. 1).

1.1. Global Cartesian coordinate system (X, Y, Z)

The global Cartesian coordinate system is used to define the nodal coordinates and the displacements. The global stiffness/mass matrices and the applied force vector are also referred to this coordinate system.

1.2. Curvilinear coordinate system (ξ, η, ζ)

The shape functions N_i are expressed in terms of the curvilinear coordinate system. The middle surface of the shell element is defined by the ξ, η coordinates. The ζ direction is only approximately normal to the middle surface and varies from -1 to $+1$ in the thickness direction.

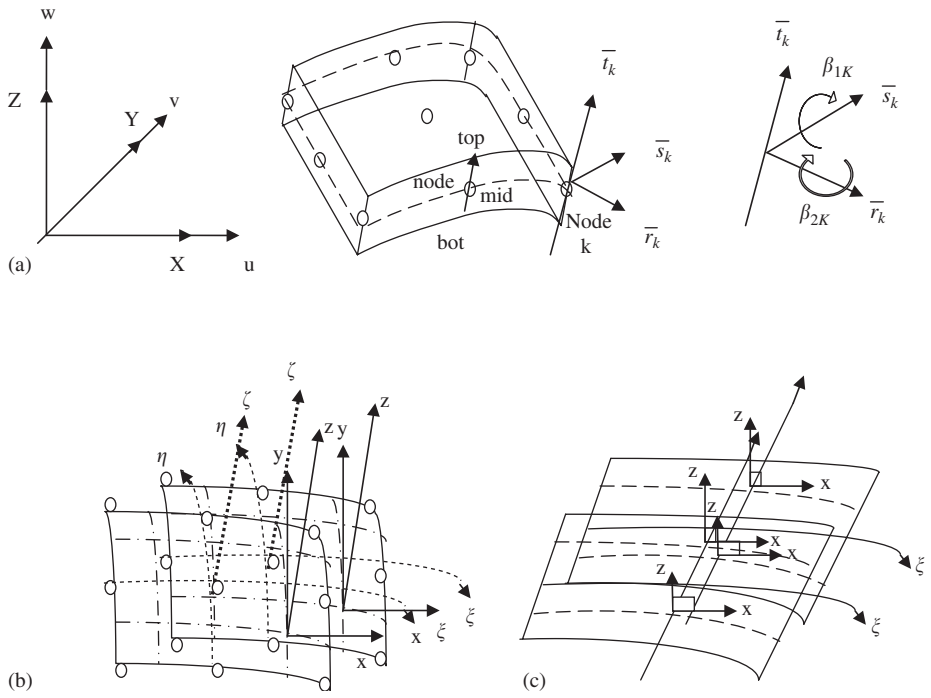

Fig. 1. Coordinate systems: (a) global and nodal coordinate system, (b) curvilinear coordinate system and local coordinate system at $\zeta =$ constant and (c) local coordinate system at $\eta =$ constant.

1.3. Local Cartesian coordinate system (x, y, z)

The local Cartesian coordinate system is used to define local stresses and strains at any point within the shell element. At such a point the z direction is taken to be normal to the surface $\zeta =$ constant. The vector $\hat{z}$ defines the z direction and is obtained from the cross product of vectors which are tangential to the ξ and η direction so that

$$\hat{z} = \{x_{,\xi}, y_{,\xi}, z_{,\xi}\} \times \{x_{,\eta}, y_{,\eta}, z_{,\eta}\}^{\mathrm{T}}. \tag{1}$$

The vector $\hat{x}$ in the x direction is taken to coincide with the tangent to the ξ direction so that

$$\hat{x} = \{x_{,\xi}, y_{,\xi}, z_{,\xi}\}^{\mathrm{T}}. \tag{2}$$

The vector $\hat{y}$ in the y direction is obtained by the cross product of $\hat{z}$ and $\hat{x}$ so that

$$\hat{y} = \hat{z} \times \hat{x}. \tag{3}$$

The local coordinate system varies throughout the shell. The direction cosine matrix $[\alpha]$ which enables the transformation between the local and global coordinate systems is defined by the expression

$$[\alpha] = [\hat{x}, \hat{y}, \hat{z}], \tag{4}$$

where $\hat{x}$, $\hat{y}$ and $\hat{z}$ are unit vectors along x, y and z, respectively.

1.4. Nodal Cartesian coordinate system ($r_k\ s_k\ t_k$)

The Cartesian coordinate system associated with each nodal point of the shell element has its origin at the shell mid-surface. The vector in the t_k direction is constructed from the nodal coordinates of the top and bottom surfaces at node k so that $t = x_k^{\mathrm{top}} - x_k^{\mathrm{bot}}$, where $x_k = [x_k,\ y_k,\ z_k]^{\mathrm{T}}$ and the vector r_k is perpendicular to s_k and parallel to the global XZ plane, so that $r_k^x = t_k^z$, $r_k^y = 0$ and $r_k^z = -t_k^x$; if t_k is coincident with the y direction (i.e. $t_k^x = t_k^z = 0$) then, $r_k^x = -t_k^y, r_k^y = r_k^z = 0$ where the superscripts refer to the vector components in the global coordinate system. The vector s_k is perpendicular to the plane defined by r_k and t_k, so that $s_k = t_k \times r_k$. The unit vectors in the directions r_k, s_k and t_k are represented by $\hat{r}_k$, $\hat{s}_k$ and $\hat{t}_k$, respectively. The vector $\hat{t}_k$ defines the direction of the normal at node k which is not necessarily perpendicular to the mid-surface at k. Vectors $\hat{r}_k$ and $\hat{s}_k$ define the rotations β_{2k} and β_{1k}, respectively.

2. Element geometry and displacement field representation

In the isoparametric formulation the coordinates of a point within the element maybe expressed as

$$X = \sum_{k=1}^{9} N_k x_k^{\mathrm{mid}} + \sum_{k=1}^{9} N_k h_k \frac{\zeta}{2} \bar{t}_k^x, \tag{5}$$

$$Y = \sum_{k=1}^{9} N_k y_k^{\mathrm{mid}} + \sum_{k=1}^{9} N_k h_k \frac{\zeta}{2} \bar{t}_k^y, \tag{6}$$

$$Z = \sum_{k=1}^{9} N_k z_k^{\mathrm{mid}} + \sum_{k=1}^{9} N_k h_k \frac{\zeta}{2} \bar{t}_k^z, \tag{7}$$

where X_k, Y_k, and Z_k are the global Cartesian coordinates of the nodal point k. $N_k = N_k(\xi, \eta)$, $k = 1, \ldots, 9$ are the 2-D shape functions corresponding to the surface $\zeta =$ constant. ξ, η and ζ are the normalized coordinates for the point under consideration. h_k is the shell thickness at node k.

As the strains in the directions normal to the mid-surface are assumed to be negligible, the displacement throughout the element will be taken to be uniquely defined by the three Cartesian components of the mid-surface node displacement and two rotations of the nodal vector t_k about orthogonal directions normal to it. The element displacement field can be expressed as

$$u = \sum_{k=1}^{9} N_k u_k + \sum_{k=1}^{9} N_k \zeta h_k \left[\bar{r}_k^x - \bar{s}_k^x\right] \begin{bmatrix} \beta_{1k} \\ \beta_{2k} \end{bmatrix}, \tag{8}$$

$$v = \sum_{k=1}^{9} N_k v_k + \sum_{k=1}^{9} N_k \zeta h_k \left[\bar{r}_k^y - \bar{s}_k^y\right] \begin{bmatrix} \beta_{1k} \\ \beta_{2k} \end{bmatrix}, \tag{9}$$

$$w = \sum_{k=1}^{9} N_k w_k + \sum_{k=1}^{9} N_k \zeta h_k \left[\bar{r}_k^z - \bar{s}_k^z\right] \begin{bmatrix} \beta_{1k} \\ \beta_{2k} \end{bmatrix}, \tag{10}$$

where h_k is the shell thickness at node k. As it is assumed that there is zero stress in the direction perpendicular to the tangent plane, i.e., $\zeta =$ constant surface, the constitutive relationship between the five stress and strain components in the local coordinate system can be written as $\{\sigma'\} = [\bar{D}]\{\varepsilon'\}$.

The stress and strain components are, respectively,

$$\sigma' = \begin{Bmatrix} \sigma_x \\ \sigma_y \\ \sigma_{xy} \\ \sigma_{xz} \\ \sigma_{yz} \end{Bmatrix} \quad \text{and} \quad \varepsilon' = \begin{Bmatrix} \varepsilon_x \\ \varepsilon_y \\ \varepsilon_{xy} \\ \varepsilon_{xz} \\ \varepsilon_{yz} \end{Bmatrix}, \tag{11}$$

$$D = \begin{bmatrix} Q_{11} & Q_{12} & & & & \\ Q_{21} & Q_{22} & & & & \\ & & Q_{33} & & & \\ & & & Q_{44} & & \\ & & & & Q_{55} & \end{bmatrix}, \tag{12}$$

$$\begin{aligned} &Q_{11} = \frac{E_L}{1 - \upsilon_{LT}\upsilon_{TL}}, \quad Q_{12} = \upsilon_{TL} \times Q_{11}, \quad Q_{22} = \frac{E_T}{1 - \upsilon_{LT}\upsilon_{TL}}, \\ &Q_{66} = G_{12}, \quad Q_{44} = G_{13}, \quad Q_{55} = G_{23}, \end{aligned} \tag{13}$$

where E_L and E_T are the longitudinal and transverse Young's moduli along the respective material axis, υ_{TL} and υ_{LT} are the Poisson's ratio in the longitudinal and transverse direction, respectively. G_{12} G_{13} and G_{23} are the shear moduli. Now,

$$\bar{D} = [T]^{\mathrm{T}}[D][T], \tag{14}$$

where $[T]$ is the transformation matrix which transforms the elasticity matrix in the material axis system to the global coordinate system.

The transformation matrix $[T]$ is given by

$$T = \begin{bmatrix} c^2 & s^2 & 2cs & & \\ s^2 & c^2 & -2cs & & \\ -cs & cs & c^2 - s^2 & & \\ & & & c & -s \\ & & & s & c \end{bmatrix}, \tag{15}$$

where $c = \cos\theta$, $s = \sin\theta$ and θ is the angle between the material axis (L,T) with respect to the global (X,Y) axis.

The strain displacement relation is given by

$$\begin{Bmatrix} \varepsilon_x \\ \varepsilon_y \\ \varepsilon_{xy} \\ \varepsilon_{yz} \\ \varepsilon_{xz} \end{Bmatrix} = \begin{Bmatrix} \dfrac{\partial u}{\partial x} \\ \dfrac{\partial v}{\partial y} \\ \dfrac{\partial u}{\partial y} + \dfrac{\partial v}{\partial x} \\ \dfrac{\partial w}{\partial y} + \dfrac{\partial v}{\partial z} \\ \dfrac{\partial u}{\partial z} + \dfrac{\partial w}{\partial x} \end{Bmatrix}. \tag{16}$$

The $\{u, v, w\}$ displacements are written in terms of $\{u_k, v_k, w_k\}$ and $\{\beta_{1k}, \beta_{2k}\}$. This leads to

$$\varepsilon = [B]\{u\}, \quad \{u\}^{\mathrm{T}} = \{u_1, v_1, w_1, \beta_{11}, \beta_{12}, \ldots, u_9, v_9 \ldots, \beta_{29}\}, \tag{17}$$

with $[B]$ representing the strain displacement matrix .

2.1. Stiffness evaluation

In the local coordinate system, the total potential energy for the degenerated shell is given as

$$\Pi = \frac{1}{2}\int_v \{\varepsilon'\}^{\mathrm{T}}[D]\{\varepsilon'\}\,\mathrm{d}V. \tag{18}$$

Upon FE discretization minimization of Π with respect to nodal variables we get in the form

$$[K]\{d\} = \{f\}, \tag{19}$$

where

$$[K] = \int [B^{\mathrm{T}}]\,[\bar{D}][B]\,\mathrm{d}V, \tag{20}$$

$[B]$ is the strain displacement matrix and $[\bar{D}]$ is the constitutive matrix.

For the analysis of composites the stiffness matrix is obtained by integrating over the thickness t. This formulation leads to shear and membrane locking when applied to thin shells, i.e., over stiff solutions are obtained due to the development of spurious transverse shear and membrane strains. To prevent this, an enhanced interpolation of the transverse shear strains in the natural coordinates ξ, η, ζ is used to produce a shear locking free element and an enhanced interpolation of the membrane strains in the local coordinates is used to produce a membrane locking free element [4]. The assumed shear and membrane strains can be defined in the following form:

$$\gamma_{\xi\zeta} = \sum_{i=1}^{3}\sum_{j=1}^{2} P_i(\eta)Q_j(\xi)\gamma_{\xi\zeta}^{ij}, \tag{21}$$

$$\gamma_{\eta\zeta} = \sum_{i=1}^{3}\sum_{j=1}^{2} P_i(\xi)Q_j(\eta)\gamma_{\eta\zeta}^{ij}, \tag{22}$$

$$\varepsilon_{rr} = \sum_{i=1}^{3}\sum_{j=1}^{2} P_i(r)Q_j(s)\varepsilon_{rr}^{ij}, \tag{23}$$

$$\varepsilon_{ss} = \sum_{i=1}^{3}\sum_{j=1}^{2} P_i(s)Q_j(r)\varepsilon_{ss}^{ij}, \tag{24}$$

$$\varepsilon_{rs} = \sum_{i=1}^{3}\sum_{j=1}^{2} P_i(r)Q_j(s)\varepsilon_{rs}^{ij}, \tag{25}$$

$$P_1(r) = \frac{1}{2}\left(1+\sqrt{3r}\right), \quad P_2(r) = \frac{1}{2}\left(1-\sqrt{3r}\right), \tag{26}$$

$$Q_1(r) = \frac{1}{2}r(r+1), \quad Q_2(r) = 1-r^2, \quad Q_3(r) = \frac{1}{2}r(r-1). \tag{27}$$

2.2. Mass matrix

The mass matrix is obtained from the kinetic energy of the system. The kinetic energy is

$$\mathrm{KE} = \frac{\rho}{2}\int (\dot{u}+\dot{v}+\dot{w})^2 \,\mathrm{d}v, \tag{28}$$

$$\mathrm{KE} = \frac{1}{2}u^{\mathrm{T}}[M]u. \tag{29}$$

The consistent mass matrix $[M]$ consists of parts corresponding to its translational and rotational dof. Assuming uniform distribution of mass, the consistent mass matrix is

$$M = \int_v [S]^{\mathrm{T}}[\rho][S]\,\mathrm{d}v, \tag{30}$$

where ρ is the density.

The 5×5 matrix ρ and the 5×45 matrix $[S] = [S^1\ S^2 - - S^9]$ are

$$\rho = \begin{bmatrix} \rho & & & \rho h & \\ & \rho & & & \rho h \\ & & \rho & & \\ \rho h & & & \dfrac{\rho h^2}{2} & \\ & \rho h & & & \dfrac{\rho h^2}{2} \end{bmatrix}, \tag{31}$$

$$[S]^i = \begin{bmatrix} N_1 & & & N_1\zeta h_1 \bar{r}_1^x & N_1\zeta h_1 \bar{s}_1^x \\ & N_1 & & N_1\zeta h_1 \bar{r}_1^y & N_1\zeta h_1 \bar{s}_1^y \\ & & N_1 & N_1\zeta h_1 \bar{r}_1^z & N_1\zeta h_1 \bar{s}_1^z \\ & & & N_1 & \\ & & & & N_1 \end{bmatrix}. \tag{32}$$

2.3. Numerical studies

Seven numerical studies have been done to investigate the accuracy and reliability of the shell element that has been developed based on the formulation that has been described in the previous sections. Results obtained using the present study have been compared with the exact and numerical solutions available in the literature. Plate and shell structures have been investigated.

2.3.1. Laminated square plate

Natural frequency analysis has been carried out for a thin laminated plate. Different lay up sequences have been investigated for the thin plate with $h/a = 0.006$. Material properties used are $E_L = 2.45E_T$, $G_{12} = G_{13} = 0.48E_T$, $G_{23} = 0.48E_T$, $v = 0.23$ and mass density $\rho = 8000$. The dimensionless frequency parameter is given by

$$\Omega = \sqrt{\frac{\rho h \omega^2 a^4}{D_0}}, \quad D_0 = E_L h^3/[12(1 - v_{12}v_{21})]. \tag{33}$$

Table 1 gives the dimensionless frequency of the plates with four edges simply supported. Table 2 gives the dimensionless frequency of the plates with four edges clamped. The full plate is modeled. The results have been compared with the solution given by Dai [6], Leissa [7] and Chow [8]. The results agree well with the results presented by them although the present formulation shows lower frequencies (about 5%) than those cases.

2.3.2. Two layered composite cylindrical panel

The panel has $R = 100\,\text{m}$ and $l = 20\,\text{m}$. Therefore $R/l = 5$. The total thickness of the panels examined are $h = 2$ and $0.2\,\text{m}$. i.e. the side length to thickness ratios are 10 and 100. All layers are of equal thickness and same material. The fiber angle orientation considered is 0/90. The material properties of the layers have the following values: $E_L = 2.5 \times 10^{11}$, $E_T = E_L/25$, $G_{12} = G_{13} = 0.5E_T$, $G_{23} = 0.2E_T$, $v = 0.25$ and mass density $\rho = 1000\,\text{kg/m}^3$. The panel is simply supported on all four edges. The full panel is modeled. The 5×5 mesh is used in the computation of the natural frequencies associated with the fundamental doubly symmetric modes. The results are compared with the solutions given by Reddy [9] and Liu [10]. Table 3 shows the dimensionless fundamental natural frequency for the doubly symmetric modes for the cylindrical panel. The results obtained by the present formulation agree well with the results of Reddy and Liu. The frequencies has been normalized using the equation

$$\beta = \frac{wl^2}{h}\sqrt{\frac{\rho}{E_t}}. \tag{34}$$

Table 1
Natural normalized frequency Ω of laminated square plates ($h = 0.06$, $h/a = 0.006$), Boundary condition: Simply supported on all sides

Ply angle	Source	Modes Ω					
		1	2	3	4	5	6
0,0,0	Present	14.06	30.08	41.12	56.17	59.72	83.42
	Dai [6]	15.19	33.30	44.42	60.78	64.53	90.29
	Leissa [7]	15.17	33.32	44.51	60.78	64.79	90.42
15/–15/15	Present	14.24	31.47	40.58	56.03	61.69	84.27
	Dai [6]	15.43	34.09	43.80	60.85	66.67	91.40
	Leissa [7]	15.40	34.12	43.96	60.91	66.92	91.76
30/–30/30	Present	14.62	32.93	39.37	56.21	66.24	79.21
	Dai [6]	15.90	35.86	42.62	61.45	71.71	85.72
	Leissa [7]	15.87	35.92	42.70	61.53	71.10	86.31
45/–45/45	Present	14.82	33.78	38.64	56.40	70.94	74.04
	Dai [6]	16.14	36.93	41.81	61.85	77.04	80.00
	Leissa [7]	16.10	37.00	41.89	61.93	77.99	80.11

Table 2
Natural normalized frequency Ω of laminated square plates ($h = 0.06$, $h/a = 0.006$), Boundary condition: Clamped on all sides

Ply angle	Source	Modes Ω						
		1		2		3	4	5	6
0,0,0	Present	26.96		47.05		62.30	79.22	80.72	109.58
	Dai [6]	29.27		51.21		67.94	86.25	87.97	119.3
	Chow [8]	29.13		50.82		67.29	85.67	87.14	118.6
15/–15/15	Present	26.76	27.8*	47.55	49.3*	61.01	77.98	83.12	109.94
	Dai [6]	29.07		51.83		66.55	85.17	90.56	120.0
	Chow [8]	28.92		51.43		65.92	84.55	89.76	119.3
30/–30/30	Present	26.37		48.98		58.01	76.99	88.12	105.62
	Dai [6]	28.69		53.57		63.26	84.43	96.15	115.5
	Chow [8]	28.55		53.15		62.71	83.83	95.21	114.1
45/–45/45	Present	26.18		50.19		56.01	76.67	94.14	97.91
	Dai [6]	28.50		55.11		60.94	84.25	103.2	106.7
	Chow [8]	28.38		54.65		60.45	83.65	102.0	105.6

*Frequencies obtained by not considering the effect of rotational component of displacement in the inertia calculation.

Table 3
Normalized fundamental natural frequencies β for doubly symmetric modes of cylindrical panel

Lamina stacking sequence	0/90	
Thickness, h (m)	2	0.2
Normalized frequency—Present (β)	9.1	17.7
Normalized frequency—Reddy [9] (β)	8.9	16.7
Normalized frequency—Liu [10] (β)	8.4	17.39

2.3.3. Thick laminated rectangular plate

The plate considered here is a rectangular carbon/epoxy plate with dimensions $150 \times 100 \times 40\,\text{mm}^3$. The fiber angle orientation of the eight layered laminate is $(0/90)_{2s}$.

The span to depth and span to thickness ratios are 1.5 and 3.75, respectively, which corresponds to a thick laminated structure. The material properties chosen are $E_L = 114\,\text{GPa}$, $E_T = 8.0\,\text{GPa}$, $G_{12} = G_{13} = 3.1\,\text{GPa}$, $G_{23} = 2.9\,\text{GPa}$, $v = 0.29$ and mass density $\rho = 1480\,\text{kg/m}^3$. The plate is free on all four edges and the full plate is modeled. The first three natural frequencies are compared with the results presented by Cugnoni [11] in Table 4. The present results show good agreement with the literature.

2.3.4. Laminated square plate for different a/h ratios

The plate considered here is a square laminated plate. The fiber angle orientations of the four layered laminate is $(0/90)_s$. The material properties are similar to the laminated rectangular plate mentioned in the above section. The plate has a thickness h and side dimension a. The span to thickness (a/h) is varying from 4 to 100. Four cases with $a/h = 4$, 10, 20 and 100 are looked investigated. The plate is simply supported on all four edges. The full plate is modeled. The natural frequencies are normalized using the equation:

$$\beta_a = \omega \sqrt{\frac{a^4 \rho}{E_t h^2}}. \tag{35}$$

Table 5 gives the dimensionless natural frequency for different a/h ratios. The results agree well with Cugnoni [11].

Table 4
Natural frequencies for laminated thick rectangular plate

Mode	Numerical results (Hz)			
	Present	Cugnoni [11] (FSDT)	Cugnoni [11] (3D)	Cugnoni [11] (HSDT)
1	3148	3045	3051	3045
2	6454	7104	7304	7113
3	7520	7819	7990	7819

Table 5
Natural frequencies for laminated thick rectangular plate

a/h	Numerical results β_a			
	Present	Cugnoni [11] (FSDT)	Cugnoni [11] (HSDT)	Carrera [12] (Closed form)
4	8.82	9.388	9.960	9.473
10	14.41	15.13	15.57	15.34
20	16.98	17.65	17.83	17.70
100	18.23	18.82	18.75	18.76

Table 6
First three natural frequencies for doubly symmetric modes of nine layered thin spherical panel

Mode λ	Present	Liu
1	67.523	67.63
2	143.07	146.97
3	184.46	171.87

2.3.5. *Layered thin spherical panel*

A nine-layered laminated composite spherical panel is considered. The panel has radius $R = 100\,\text{m}$ and side length $l = 1\,\text{m}$. The thickness of the panel is $h = 0.01$. Fiber angle orientation is (0/90/0/90/0/90/0/90/0). The material for all the layers are graphite/epoxy composite having $E_L = 2.0685 \times 10^{11}$, $E_T = E_L/40$, $G_{12} = G_{13} = 0.5\ E_T$, $G_{23} = 0.6\ E_T$, $v = 0.25$ and mass density $\rho = 1605\,\text{kg/m}^3$. The panel is clamped on all four edges. The full panel is modeled. The natural frequencies are normalized using the equation:

$$\lambda = \frac{wl^2}{h}\sqrt{\frac{\rho}{E_t}}. \tag{36}$$

Table 6 gives the first three normalized natural frequencies for the doubly symmetric modes of nine-layered spherical panel. The present results agree well with the solutions given by Liu [10]. The first eight mode shapes for the layered spherical panel are shown in Fig. 2. A convergence study has been done for this case. A 2×2, 5×5, 8×8 and 15×15 mesh have been examined. It can be found from Table 7 that the results are converging with the increase in mesh size.

Rotational components of the displacement are modeled to obtain the inertia effects, which could explain the fact that the frequencies predicted by the present formulation are always on the lower side, when benchmarked with the literature. When they are neglected the frequencies increase as seen for one sample case in Table 2. These effects are more significant in thin shells when compared to thick shells.

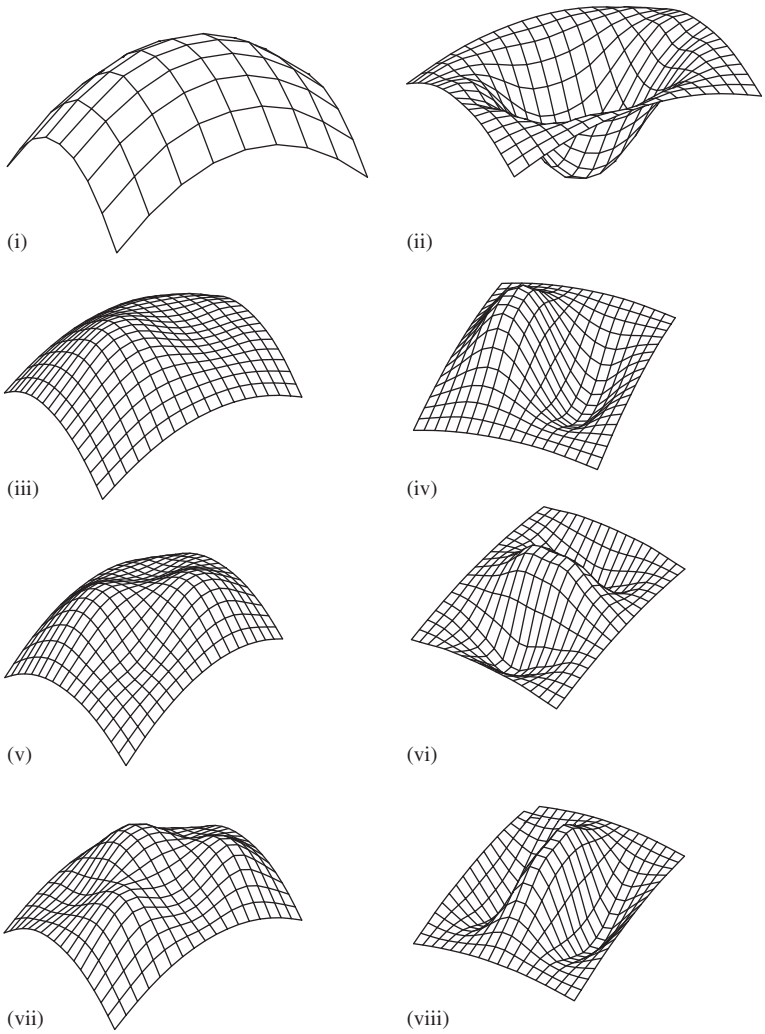

Fig. 2. (i) Spherical panel. (ii)–(viii) Mode shapes for nine-layered spherical panel.

Table 7
Convergence study for nine layered spherical panel

Mesh	Normalized natural frequency λ			
	Mode 1	Mode 2	Mode 3	Mode 4
2×2	71.14	106.80	131.40	155.32
5×5	67.78	84.78	100.63	114.94
8×8	67.44	84.24	99.84	113.86
15×15	67.43	84.16	99.71	113.70

3. Conclusions

A nine-node degenerate shell element has been developed for the free vibration analysis of laminated composite. The shell element works for both thick and thin shells. An enhanced interpolation of the transverse shear strains in the natural coordinates is used in this formulation to produce a shear locking free element and an enhanced interpolation of the membrane strains in the local coordinates is used to produce a membrane

locking free element. The interpolation functions used in formulating the assumed strains is based on the Lagrangian interpolation polynomials. Numerical studies have been done to investigate the accuracy and reliability of the shell element that has been developed based on the formulation that has been described in the previous sections. Several numerical examples are presented for laminates with different side to thickness ratios, material properties, boundary conditions and ply angles. Results obtained using the present study has been compared with the exact and solutions available in the literature. Transverse rotary inertia effects are modeled, which could explain the fact that the frequencies predicted by the present formulation are always on the lower side, when benchmarked with the literature. These effects would be significant in thick shells. It was seen that the results obtained using the present formulation shows good agreement with the results available in the literature which illustrate the robustness and efficiency of the present method.

Acknowledgment

The authors would like to thank the Naval Research Board (NRB), India for supporting this investigation.

References

[1] S. Ahmad, B.M. Irons, O.C. Zienkiewicz, Analysis of thick and thin shell structures by curved finite elements, *International Journal of Numerical Methods in Engineering* 2 (1970) 419–451.
[2] O.C. Zienkiewicz, R.L. Taylor, J. M Too, Reduced integration techniques in general analysis of plates and shells, *International Journal of Numerical Methods in Engineering* 3 (1971) 575–586.
[3] S.F. Pwasey, R.W. Clough, Improved numerical integration of thick shell finite elements, *International Journal of Numerical Methods in Engineering* 3 (1971) 575–586.
[4] H.C. Huang, E. Hinton, A new nine node degenerated shell element with enhanced membrane and shear interpolation, *International Journal of Numerical Methods in Engineering* 22 (1986) 73–92.
[5] S.J. Lee, S.E. Han, Free-vibration analysis of plates and shells with a nine-node assumed natural degenerate shell element, *Journal of Sound and Vibration* 241 (4) (2001) 605–633.
[6] K.Y. Dai, G.R. Liu, K.M. Lim, X.L. Chen, A mesh free method for static and free vibration analysis of shear deformable laminated composite plates, *Journal of Sound and Vibration* 269 (2004) 633–652.
[7] A.W. Leissa, Y. Narita, Vibration studies for simply supported symmetrically laminated rectangular plates, *Composite Structures* 12 (1989) 113–132.
[8] S.T. Chow, K.M. Liew, K.Y. Lam, Transverse vibration of symmetrically laminated rectangular composite plates, *Composite Structures* 20 (1992) 213–226.
[9] J.N. Reddy, Exact solutions of moderately thick laminated shells, *ASCE Journal of Engineering Mechanics* 110 (4) (1984) 794–809.
[10] C.W.S. To, B. Wang, Hybrid strain-based three-node flat triangular laminated composite shell elements for vibration analysis, *Journal of Sound and Vibration* 211 (1998) 277–291.
[11] J. Cugnoni, Th. Gmur, A. Schorderet, Identification by model analysis of composite structures modeled with FSDT and HSDT laminated shell finite elements, *Composites: Part A Applied Science and Manufacturing* 35 (2004) 977–987.
[12] E. Carrera, An assessment of mixed and classical theories on global and local response of multilayered orthotropic plates, *Composite Structures* 50 (2) (2000) 183–198.